International Journal of Latest Trends in Engineering and Technology
Special Issue AFTMME-2017, pp. 141-151
e-ISSN:2278-621X

ANALYSIS OF OXIDATION BEHAVIOR OF NANOSTRUCTURED ALCRN AND TIALN COATINGS ON SA213T91 BOILER STEEL

Lucky Goyal[1], Vikas Chawla[2] & Jasbir Singh Hundal[3]

Abstract- The oxidation of Nanostructured AlCrN and TiAlN coatings on T91 boiler steel subjected under cyclic conditions has been investigated. Surface and cross sectional analysis has been done with SEM/EDS and XRD techniques to know the corrosion kinetics and its mechanism. TiAlN coated specimen has shown higher surface and internal oxidation as well as weight gain. Comparatively, the excelling performance of AlCrN coating has been observed by virtue of low internal oxidation as well as Cr and Al availability in the oxide scale to form protective corrosion barriers.
Keywords: Oxidation, AlCrN, TiAlN, SEM/EDS, XRD

1. INTRODUCTION

Degradation of metals at high temperature has been observed to be an imperative issue in various high temperature operations as in steam generators, turbines, engines and industrial incinerators etc. [1]. Tubes of steam generators have shown degradation due to elevated temperature exposure. Reportedly methods have been studied and recommended to curb the high temperature degradation of materials [2]. The components of boiler have frequent failures by virtue of overheating, erosion, corrosion or other factors [3]. High temperature corrosion of structural materials in coal-fired boilers, in particularly of heat exchanger tubes, has become a very important issue in the design and operation of thermal power plants and is recognized as one of the main cause of down time in these installations [4]. Various impurities such as S, V and Na are available in the fuel used in the boilers of power plants [5]. At elevated temperature, they react with each other and form low melting eutectic mixture of Na_2SO_4 - 60%V_2O_5. These compounds commonly known as ash, deposit on the surface of the materials and induce corrosion.

The application of protective coatings can impart high temperature resistance to the materials exposed to above said environment [6]. The primary aim of the coating/surface treatment is the ability to produce a stable, slow-growing surface oxide providing a barrier between the coated alloy and the environment [7].Nanostructured materials have different behaviour than their macroscopic counterparts by virtue of their smaller size [8]. Nanostructured coatings employing nanostructured materials (referred to grain size < 100nm) have attracted the interest of many researchers [9, 10] by virtue of better features as higher ductility, hardness, wear & corrosion resistance than the conventional coatings [11, 12]. Transition metal nitride coatings are now a day's widely used in wear and corrosion protection applications just as for cutting tools, forging and dies operating at elevated temperature [13]. The nanostructured coatings have been reported to have better corrosion resistance due to low porosity and expanded grain boundary. Secondly, due to higher grain boundary the denser oxide scale get formed in the scale [14]. Kumar et al. [2] have observed better corrosion resistance of nanostructured Ni-Cr coatings on T91 boiler steel than their conventional counterparts. Reportedly oxidation degradation of thin films coated on cutting tools has been studied. It is reported that addition of Al to CrN to produce AlCrN coatings can enhance the corrosion resistance of the coating. Production of (Cr, Al)$_2O_3$ oxide layer developed during initial stages of corrosion have the capacity to act as an effective diffusion barrier for inward movement of corroding species at elevated temperature [13].

Limited information regarding the degradation mechanisms of nanostructured coatings at elevated temperature has been reported in detail so far [15]. An investigation regarding the high temperature cyclic study of nanostructured TiAlN and AlCrN coatings on T91 boiler steel in an aggressive molten salt environment of Na_2SO_4-60%V_2O_5 at 900^{0}C has been studied. Austenitic T91 steel is extensively used boiler steel for power plant boiler components, mainly in the super heater zone having deteriorated by virtue of erosion and corrosion issues [16]. The imposed cyclic conditions refer to the most realistic industrial environment [17]. The hot corrosion environment of Na_2SO_4-60%V_2O_5 has been selected to simulate the actual conditions of the molten sulphate-vandate deposits resulting from the condensation of combustion products of low-grade fuels [18]. The imposed temperature i.e. 900^{o}C invokes most aggressive attack on the metals [19]. The information of investigations will be useful to explore the possibility of usefulness of thin nanostructured coatings on the boiler tubes.

2. MATERIALS AND METHODS

2.1 Preparation of specimens

[1] Research Scholar, I. K. Gujral Punjab Technical University, Kapurthala, Punjab, India
[2] Professor, I. K. Gujral Punjab Technical University, Kapurthala, Punjab, India
[3] Registrar, Maharaja Ranjit Singh Punjab Technical University, Bathinda, Punjab, India

In the present research, T91 boiler steel (SA213T91) was used as the substrate material for the study. T91 boiler steel is normally used in the components of the power plants, operated at the higher temperature. The material was procured from Guru Nanak Dev Thermal Plant, Bathinda, Punjab, India. The chemical composition of the substrate is as given in Table 1. Although T91 boiler steel has adequate mechanical strength at elevated temperature, often it lacks resistance to oxidizing or corroding environments during longer periods of usage [20]. The specimens with dimensions of approximately 20mm x 15mm x 3.5mm were prepared out of the boiler tube. The specimens were polished using emery papers of 220, 400, 600 grit sizes and subsequently on 1/0, 2/0, 3/0 and 4/0 grades. Then the samples were mirror polished using cloth polishing wheel machine with lavigated alumina powder suspension. The samples were prepared manually and care was taken to avoid any structural changes in the samples.

Table 1 Chemical composition (wt. %) of the T91 boiler steel.

Substrate	C	Cr	Mn	Mo	Si	V	Nb	Fe
T91	0.0964	8.75	0.478	1.04	0.36	0.27	0.09	Balance

2.2 Details of nanostructured coatings

All the substrates have been cleaned in two steps: firstly with Ultrasonic Pre-cleaner and secondly with ultrasonic cleaning machine with 9 Tanks including hot air dryer for 1.5 Hrs. The nanostructured thin coatings namely Balinit futura nano i.e TiAlN coating and Balinit alcrona pro (AlCrN) coatings with a thickness around 4 µm were deposited on the substrate at Oerlikon balzars coatings (India) limited, Gurgaon, India. For all coatings argon (Ar) and pure nitrogen atmosphere were used during deposition. The coating parameters for all the substrate has been optimized by oerlikon balzars coatings (India) limited, Gurgaon, India. A front loading balzars rapid coating system (RCS) machine was used for the deposition of the coatings. The details of the composition of the targets, coating thickness and the summary of the process parameters are presented in Table 2.

Table 2 Summary of Nanostructured thin coatings deposition parameters

Coating Parameters	Nano Structured TiAlN	Nano Structured AlCrN
Machine Used	Standard balzers rapid coating system (RCS) Machine	Standard balzers rapid coating system (RCS) Machine
Made In	Oerlikon balzers, Swiss	Oerlikon balzers, Swiss
Target Composition	Ti, Ti_{50} Al_{50}	$Al_{70}Cr_{30}$
No. of Targets	Ti(02), $Ti_{50}Al_{50}$(04)	$Al_{70}Cr_{30}$(06)
Target Power	3.5 KW	3.5 KW
Reactive Gas	Nitrogen	Nitrogen
Deposition Pressure	3.5 Pa	3.5 Pa
Substrate Bias Voltage	-40V to -170V	-40V to -170V
Coating Thickness	4µm +1µm	4µm +1µm

2.3 Characterization of Coatings

The apparent surface porosity of the as coated specimens were measured by an Image analyzer system from Chennai Metco Pvt. Ltd. using Envision 3.0 software based on ASTM 276. X-Ray Diffraction set up of PAN Alytical Make having X'Pert PROMPD model was used to perform XRD scans along the specimen.

Scanning electron microscope (SEM) from JEOL Japan make, bearing model JSM-6610LV equipped with EDS of oxford Instrument Company was used to study the samples. The SEM micrographs with chemical analysis at different points along the substrate/ coating/ oxide layer interface were taken to know the elemental changes after hot corrosion. The surface morphology (2D & 3D) of the thin films was also characterized by AFM (Model: INTEGRA, NT-MDT, Ireland) to calculate the surface roughness and particle size. After surface characterization, the samples were sectioned with a diamond cutter (DUCOM's precision diamond saw, Model ISOMET 1000, made in USA) across its cross section and subsequently mounted in epoxy powder by using the cold mounting method. Thereafter the samples were mirror polished and gold coated to facilitate elemental analysis by SEM/EDS for various elements present across the cross-section of the substrate, coating and scale. The cross-sectional SEM micrographs with elemental variations from alloy substrate to outer scale at different points were taken to understand the movement of various elements across the substrate/ coating/ scale interface.

2.4 Air oxidation

Cyclic air oxidation studies have been done for 50 cycles. Each cycle consists of one hour heating at 900^{o}C in a silicon carbide tube furnace followed by 20 minute cooling at room temperature. The enforced cyclic pattern was used to impose stern testing environments which may testify more practical approach for observing the issue of corrosive deterioration in boiler applications [21, 22]. These studies were accomplished for 50 cycles as this length is considered to be acceptable to have the study state of oxidation, applicable to large group of materials [23, 24]. The experimental investigations were executed for the bare as well as coated specimens for comparison. The furnace was automatically calibrated by the PLC based controller having an accuracy of +5^{0}C by utilizing Pt/ Pt-13% Rh thermocouple. The physical dimensions of the

specimen were recorded carefully with a digital vernier caliper (Mitutoyo, Japan make, resolution 0.01 mm) to evaluate surface areas.

The samples were dehydrated at 100^0C for 4-5 hours in the oven to extract the moisture. The weight of these dehydrated samples, placed in the alumina boat, was weighed ahead of the hot corrosion studies. During the cyclic study, the combined weight of boat and sample was taken after the completion of each cycle with a digital balance (Model 052C citizen, India) having precision of 1 mg. The spalled and sputtered oxide debris on the samples, during the experimentation was also comprised to measure weight change. Data captured during each cycle is worked upon for calculating the corrosion kinetics. Visual observations were also made after the end of each cycle with regard to lusture, color, adherence/ spallation tendency and any other physical aspect of the oxide scales/coatings. After the oxidation studies, the corroded samples were analyzed from surface as well as cross-section with XRD and SEM/EDS techniques (point wise analysis and microanalysis mapping). The kinetics of the oxidation of the coated and bare specimen was determined using thermogravimetric analysis and by evaluating the parabolic rate constants.

3. RESULTS AND OBSERVATIONS

3.1 Surface Analysis of the as Coated Specimens

The as coated nanostructured TiAlN coating has grey, where as AlCrN coating has light grey color. Visual observations of micrographs of both as coated nanostructured coatings indicate smooth and dense surface having minor pores and inclusions. Cross-sectional SEM images of as coated nanostructured TiAlN and AlCrN coating on T91 boiler steel are presented in Fig. 1(a, b). TiAlN coating has a very fine layer of coating with structured layers embedded parallel to the substrate/coating interface. AlCrN coating also has very fine layer. The coating is intact and bounded firmly with the substrate. The porosity for as coated nanostructured TiAlN and AlCrN coatings is observed to be 0.41% & 0.42% respectively below the prescribed value (0.45%). XRD patterns of as coated TiAlN and AlCrN coatings on T91 substrate are depicted in Fig. 2. XRD analysis for TiAlN coating shows the presence of TiN and AlN phases. Further, in case of AlCrN coating the main phases are CrN and Al (Fig. 2).

Fig.1: SEM micrograph along the cross-section of as coated nanostructured (a) TiAlN and (b) AlCrN coatings on T91 boiler steel

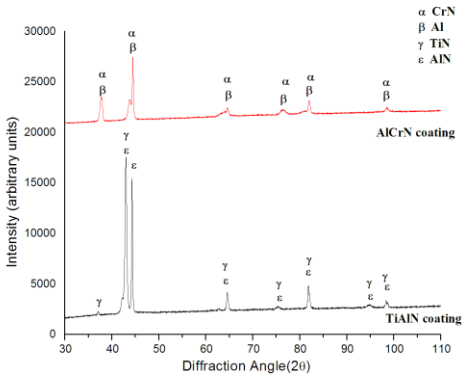

Fig. 2: XRD patterns of as coated nano-structured TiAlN and AlCrN coatings on T91 boiler steel

3.2 Surface Morphology of as Coated Specimen

SEM micrographs along with EDS analysis of as coated TiAlN and AlCrN coatings on T91 boiler steel are shown in Fig. 3(a, b). SEM micrograph of TiAlN coating has indicated dense structure with regular morphology. The EDS point analysis (Fig. 3a) shows the presence of Ti (39.39%), Al (29.36%) and N (31.25 %) elements. Absence of other elements certifies non diffusion of other elements from substrate to coating as also reported by Chawla et al. [25]. Further in case of AlCrN coating, Al (31.23%), N (33.77%) and Cr (35.00%) are the main elements as indicated by the SEM/EDS point analysis (Fig. 3b). AlCrN coating has dense grey color with tiny dark grey particles dispersed in the matrix. Surface morphology of the nanostructured TiAlN and AlCrN coated surfaces has been shown in Fig. 4 as observed by AFM (2D and 3D). Surface micrographs are also captured with FESEM facility to recuperate the nano size of the particles (Fig. 5).

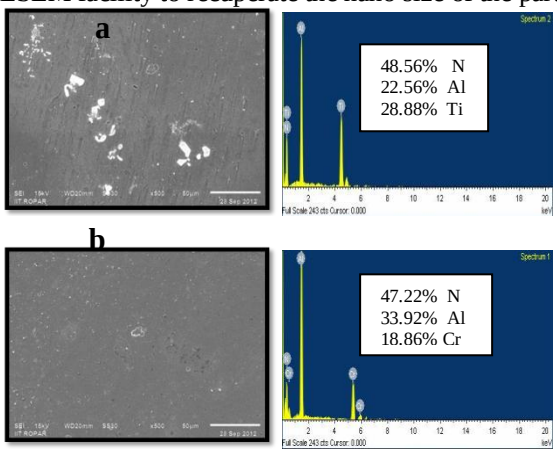

Fig. 3: Surface SEM/EDS analysis of (a) TiAlN and (b) AlCrN as coated T91 boiler steel

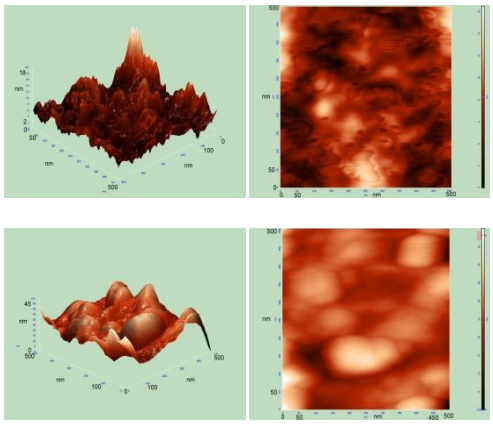

Fig. 4: 3D and 2D AFM images of as coated (a) TiAlN and (b) AlCrN on T91 boiler steel

3.3 Cyclic Oxidation studies

The T91 BM has remained unaffected during early period of the cycles i.e. up to 7th cycle. Powdered grey scale has been seen on the sample after 13th cycle, which has continuously grown till 25th cycle. Ultimately after complete study, grey scale surface with some thickness has been seen on the surface. The cyclic hot corrosion study of TiAlN coated T91 boiler steel has initially shown violet color, which changed to blackish grey color in the following cycles. No spalling of scale has been seen on the surface of TiAlN coated sample after 22nd cycle. Minor violet colored scale was seen after 26th cycle. After complete cycles the sample has developed scale with some thickness. In case of AlCrN coated T91 specimen, no scale was seen over the surface by the end of 18th cycle. Minor powdered and uniform scaling was seen on the specimen after complete study.

The graph between weight change vs number of cycles for uncoated and coated T91 boiler steel specimen subjected to air oxidation at 900^{o}C for 50 cycles is presented in Fig. 6(a). The cumulative weight gain after complete cyclic study are observed to be 41.427, 7.430 and 2.960 mg/cm^2 for T91 bare, TiAlN and AlCrN coated T91 boiler steel. The (weight gain/unit area)^2 plot against number of cycles is shown in Fig. 6b. It further confirms that parabolic law is followed by the all the three specimens. The values of parabolic rate constant (K_p) are observed to be 96.78, 3.267 and 0.378x10^{-10} g^2 cm^{-4} s^{-1} for T91 bare, TiAlN coated 347H and AlCrN coated T91oxidised in air respectively.

3.4 XRD Analysis of the Scale

XRD patterns for bare and coated T91 boiler steel specimen after 50 cycles have shown Fe_2O_3 as the major and Cr_2O_3 as the minor phase (Fig. 7). In the case of TiAlN coated specimen Ti_2O_3, NiO, Cr_2O_3 and CrN are the main phases along with the minor presence of Al_2O_3 and Fe. XRD patterns of AlCrN coated specimen have Cr_2O_3, Fe_2O_3, Al_2O_3, CrN and AlN as the major phases and minor phases respectively.

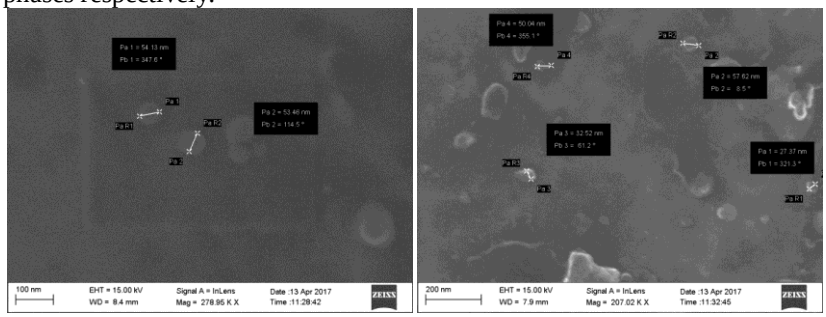

Fig. 5: FESEM Images of (a) TiAlN and (b) AlCrN coatings

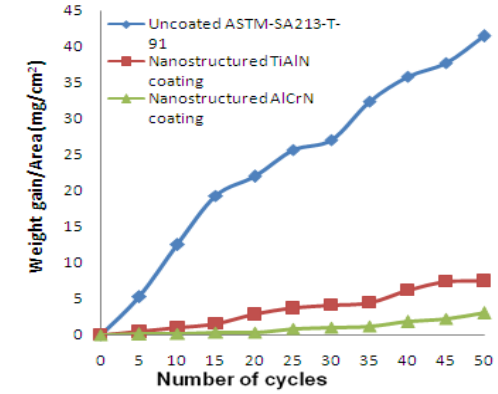

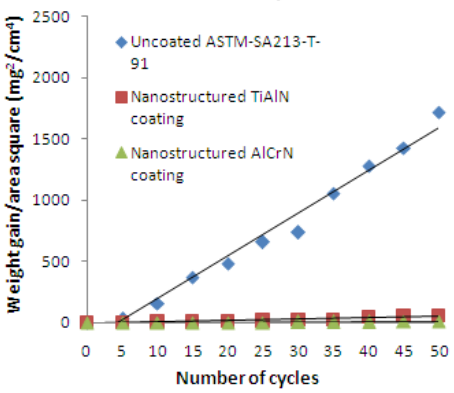

Fig. 6: wt. gain per unit area vs no. of cycles and (wt. gain/ unit area)^2 vs no. of cycles plots for coated and uncoated T91 specimens after complete cyclic study in air at 900^{o}C

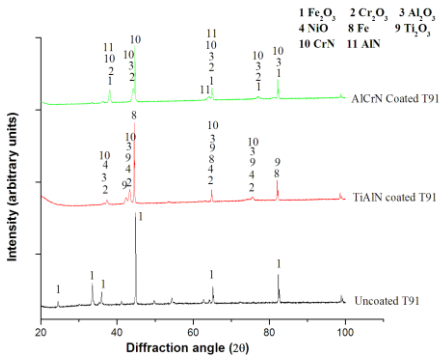

Fig. 7: XRD patterns of T91 bare, TiAlN and AlCrN coated T91 specimens after complete cyclic study in molten salt environment (Na_2SO_4-60% V_2O_5) at 900^{o}C

3.5 SEM/EDS analysis

3.5.1 Surface Analysis of the Scale

The SEM micrographs depicting the surface morphology of the specimen (bare and coated) after complete cyclic study have been presented in Fig. 8. The EDS analysis of T91 bare boiler steel has shown significant amount of Fe and O throughout the substrate, showing mainly the formation of Fe_2O_3. The EDS analysis of the scale over the surface of TiAlN coated T91 boiler steel has indicated the presence of Al, Ti, O as well as Fe, Si, Cr and Mo thereby suggesting the formation of Ti_2O_3, NiO, Cr_2O_3 and CrN. The EDS analysis of AlCrN coated T91 steel has the presence of Cr, Al and O along with minor value of Fe, Mn, Si validating the formation of Cr_2O_3, Al_2O_3, Fe_2O_3, CrN as major one and AlN as minor phases. The oxide morphology of TiAlN and AlCrN coatings has been observed to be regular and uniform.

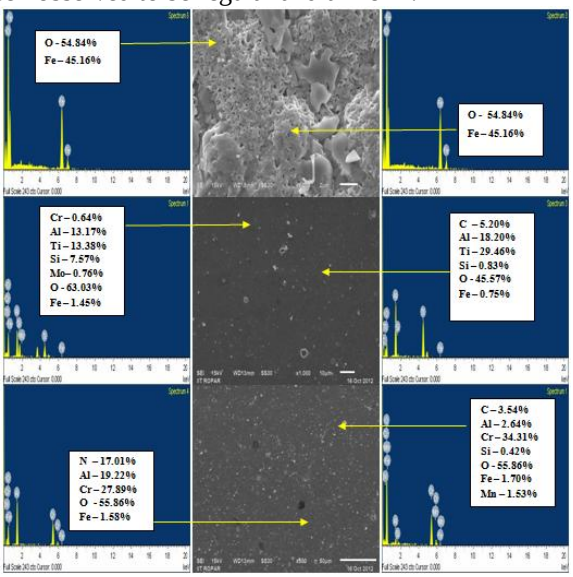

Fig.8: Surface SEM/EDS analysis for (a) T91 bare boiler steel (b) TiAlN coated T91 boiler steel and (c) AlCrN coated T91 boiler steel subjected to air oxidation at 900^{o}C after 50 cycles

3.5.2 Cross Sectional analysis of the scale

Cross-sectional SEM/EDS point analysis was observed for bare and coated T91 boiler steel at various points of interest along the cross section of oxidized and presented in Fig. 9. The cross-sectional SEM micrograph with elemental variations from alloy substrate to outer scale at different points of T91 bare specimen (Fig. 9a) indicates separated and cracked scale having higher presence of Fe and O along with minor presence of Cr, which may have reacted to form Fe_2O_3. The scale has large cracks parallel to the substrate/scale interface and observed to be exfoliated.

The cross-sectional SEM micrograph of TiAlN coated T91 boiler steel has indicated mainly presence of Ti, Al, Cr and O in the oxide area (points 7, 8, 9 and 10). The most of the oxide scale has been falling due to exfoliation and spalling (Fig. 9b). TiAlN coating has been observed to be detached and removed from the substrate after complete cyclic studies. The oxide scale for AlCrN coated T91 has been seen to be adherent without any damage to the interface between substrate and scale (Fig. 9c). The scale contains higher presence of Al, Cr, N and O along with minor values Fe indicating major presence of

Al_2O_3, Cr_2O_3 and their spinals. The oxide region of AlCrN coated T91 is comparatively richer in Cr and Al than TiAlN coated sample.

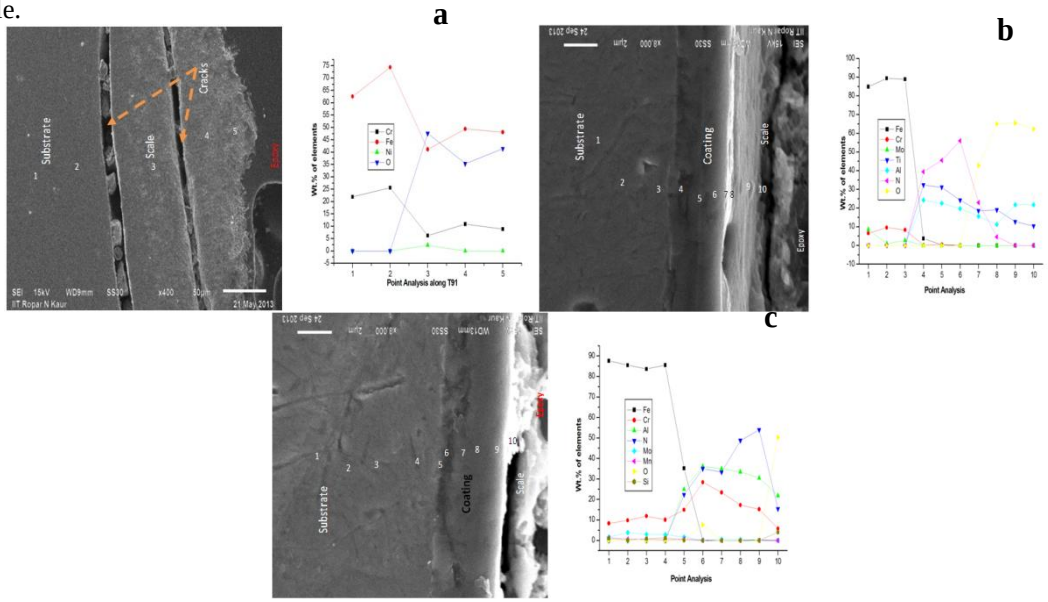

Fig. 9: Cross sectional SEM/EDS and point analysis (a) T91 bare (b) TiAlN Coated T91 boiler steel and (c) AlCrN Coated T91 boiler steel of hot corroded samples after complete cyclic study

3.6 X Ray Mapping Analysis

The compositional SEM image and x-ray mapping of the cross-section of T91 bare boiler steel after oxidation have been presented in Fig. 10a. Higher corrosion attack at the substrate/scale was seen due to loosely bound scale. Higher availability of oxygen and iron has been seen in the cracked and porous scale. The inward diffusion of oxygen has caused the deep corrosion and internal precipitation.

X-ray mapping of the TiAlN coated T91 boiler steel has presented adhered status of the coating (Fig. 10b), but the scale has been observed to be exfoliated. The scale mainly has the presence of Al, N, Ti and O along with the minor presence of Fe. The availability of Ti, Al and N has been seen in the coating.

X-ray mapping of the cross-section of oxidised AlCrN coated T91 boiler steel has shown adherent and firmly bounded coating even after complete cyclic study (Fig. 10c). Coating as well as scale has abundant presence of Al, Cr, and N along with presence of oxygen in the scale confirming the formation of Cr_2O_3, Al_2O_3, $NiCr_2O_4$ and Fe_2O_3. Comparatively, meager amount of Fe and O has been observed in the oxide scale.

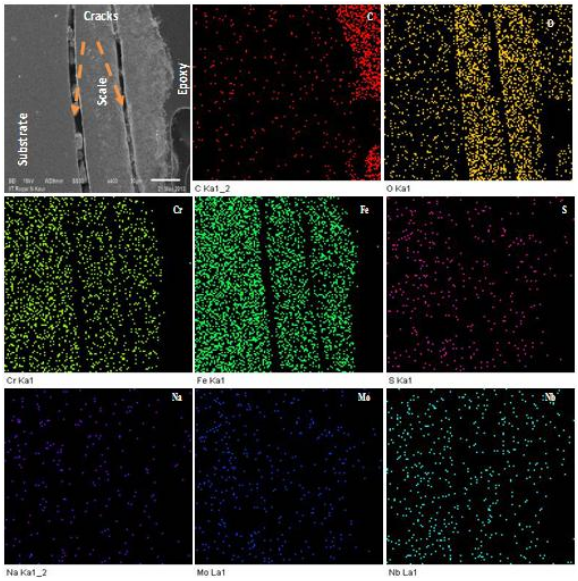

Fig. 10a: Compositional SEM Image and X-ray mapping of the cross-section of hot corroded T91 bare boiler steel at 900^0C after complete cycles

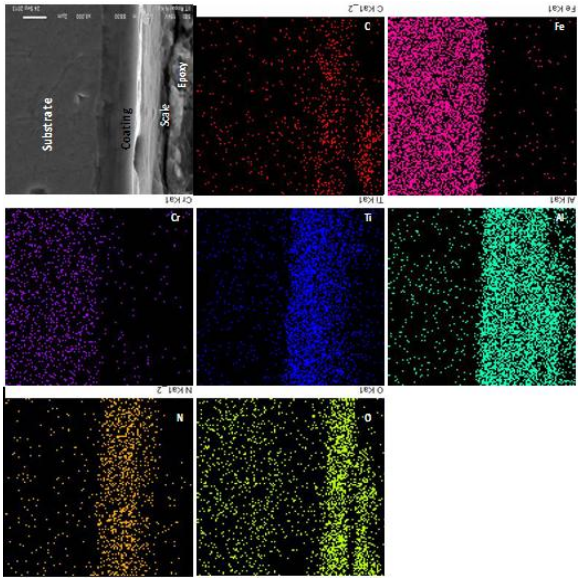

Fig.10b: Compositional SEM Image and X-ray mapping of the cross-section of hot corroded TiAlN coated T91 boiler steel after complete cyclic study.

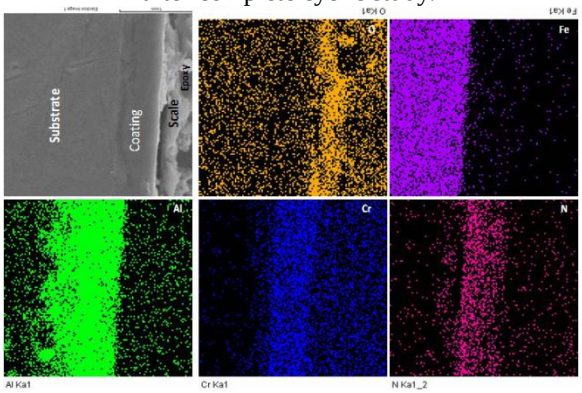

Fig. 10c: Compositional SEM Image and X-ray mapping of the cross-section of hot corroded AlCrN coated T91 boiler steel after complete cyclic study

4. DISCUSSION

As per weight change plot (Fig. 6a), both the coatings have followed the parabolic law, which rectifies the diffusion barrier role of scale. AlCrN coating has been successful to reduce the corrosion rate of T91 steel by 92.85% in the form of overall wt. gain, whereas reduction was 82.06% for TiAlN coated T91. The weight of T91 bare boiler steel has increased continuously till the end of the cyclic study bearing initial weight gain to be more till 25th cycle. The corrosion of T91 substrate has been due to nucleation and fast development of oxide scale layers. The weight change (increase) in the case of TiAlN coated T91 boiler steel is high, where as the weight gain for AlCrN coated T91 boiler steel is comparatively low, constant and gradual (Fig. 6a). The observed higher weight gain during initial cycles of study for all the specimens can be by virtue of dense and high oxide formation in the pores and vacancies of the coatings and the bare substrate. Subsequently these developed oxides restrict further movement of oxidizing elements. The rapid increase in weight gain during initial hot corrosion cycles is also reported by Mittal & Sidhu [1] and UI-hamid [27]. The parabolic rate constant has been found to be least for AlCrN coating ($K_p = 0.378x10^{-10} g^2cm^{-4}s^{-1}$). It can be depicted from the K_p values and cross sectional status of the oxidized specimen that AlCrN coatings has provided adequate protection against the corrosion to the substrate (Fig. 9c). The scale over AlCrN and TiAlN coatings has been intact, firm and adhered but in the case of TiAlN coating, the scale has been observed to be more exfoliated and removed from the substrate. The developed scale in the case of TiAlN coating was weak, porous and non-uniform (Fig. 9b). The oxide scale developed on T91 bare substrate is fragile, porous with cracks having poor adhesion (Fig. 9a).

The surface scale of T91 bare substrate has corrugated morphology (Fig. 8a). SEM micrograph of T91 bare substrate has lumps of pored scale giving enlarged surface area for exposure (Fig.8a). The surface scale over TiAlN coating is uniform having high presence of oxygen (Fig. 8b). The surface scale over AlCrN coating has regular and uniform scale, designating and validating higher amount of Cr, Al, N and O as also observed in Fig. 8c [28]. The validative presence of Cr_2O_3 and Al_2O_3 with relatively compact plate like morphology was observed over most part of the surface area (Fig.7, 8c). Similar

morphological inputs of Cr_2O_3 were also reported by Ding [29]. The morphology in SEM micrograph has indicated existence of Cr, Al and O together, directing the formation of Cr_2O_3 and Al_2O_3 (Fig. 7, 10c).

T91 bare substrate has developed fragile scale with cracks developed parallel to the substrate/scale interface (Fig.9a). These observed cracks can provide direct access of the substrate to the oxidative environment. The interface of substrate with scale was deeply exfoliated and oxygen was observed to be penetrated in the T91 substrate. The surface (Fig.8a) and cross-sectional (Fig.9a) SEM/EDS analysis has indicated higher value of Fe and O in the oxide scale, justifying the formation of Fe_2O_3 as the major phase (Fig.7). Formation of Fe_2O_3 and Cr_2O_3 in the scale has been validated in XRD analysis (Fig.7) and X-ray mapping (Fig.10a). The spalling and sputtering of scale from T91 bare steel can be due to strain developed due to precipitation of Fe_2O_3 from the liquid phase during cooling period of thermal cycle and inter diffusion of intermediate layers from oxide [31]. The availability of Fe_2O_3 in the oxide scale has been reported to be non-protective [32, 33].

The better performance of AlCrN coating has been observed by virtue of adherent oxide scale even after complete cyclic study and formation of Cr_2O_3, Al_2O_3 and CrN phases as supported by surface (Fig. 8c) and cross-sectional (Fig. 9c, 10d,e) SEM/EDS of corroded AlCrN coated T91 boiler steel. The observed phases are reported to be protective to the corrosion attack [34, 35]. Cr is reported to have high affinity towards oxygen to form Cr_2O_3 during early period of oxidation [35, 36]. The oxidation resistance of AlCrN coating is primarily dependent on the oxides of Al and Cr i.e. Al_2O_3 and Cr_2O_3, and these oxides are reported to act as protective barriers during oxidation [17, 38]. Cr_2O_3 and Al_2O_3 are thermodynamically stable phases by virtue of their high melting point [17], Al_2O_3 has been reportedly slow in progressive formation and is stable even above 1000^0C [37]. Major peaks of Cr_2O_3 were seen in the XRD (Fig. 7) of AlCrN coating, generally phases of Al_2O_3 developed a bit easier and earlier than Cr_2O_3 due to low Gibbs free energy [13]. The inculcation of Al_2O_3 in scale is observed to provide long term oxidation resistance to the alloy at elevated temperature [39]. These oxides form adherent, continuous and densely populated scale. The continuously thick and protective Cr_2O_3 and Al_2O_3 oxides in AlCrN coated T91 will not allow further transport of oxidizing species and ions. The oxide scale developed on AlCrN coating may have inhibited the further corrosion process. Chromia (Cr_2O_3) is reported to be the best option to resist the hot corrosion by virtue of preferential reaction with O^{2-} to produce the chromate [40]. The chromate is known to protect the dissolution of protective scale by stabilizing the melt [28]. The addition of Al to CrN can improve the oxidation resistance by the presence of thermally stable FCC-AlN bonds and formation of dense $(Al,Cr)_2O_3$ oxide layer on the coating surface [41]. Reportedly AlCrN coating also has good thermal stability up to 900^0C until the precipitation of h-AlN starts. Afterwards the AlCrN coating degenerates by virtue of loss of nitrogen and Cr_2N and Cr phases [41].

Comparatively very low value of Fe has moved from T91 substrate through AlCrN coating to oxide scale (Fig. 10c). Oxygen has penetrated in the AlCrN coating, but barely reached the T91 substrate, which justifies its betterment. TiAlN coating was not that much deteriorated and exfoliated to have very high corrosion rate. The stress formation during oxidation can de-laminate the oxide layer from the TiAlN coating by virtue of variations in thermal expansion coefficients of coating/oxide scale/substrate [39, 42]. The minor protective nature of TiAlN coating can be by virtue of production of NiO and Cr_2O_3 phases etc. Chim et al. [43] has also observed the complete de-lamination of the TiAlN coating during annealing at 800^0C.

Ti has been reported to produce a porous and non-protective oxides scale [44]. Kazuhis Fujita has also suggested the possible formation of porous TiO_2 and Al_2O_3 with domination of TiO_2 during oxidation [45]. The titanium based coatings are quoted to exhibit the lowest oxidation resistance [45]. Ultimately, oxides layers over the surface of TiAlN coating has decomposed as the TiAlN coating has failed during the study. There is a wide gap in the coefficient of thermal expansion of Ti, Al and Ti oxides from T91 substrate, which can direct the removal of coating and formation of cracks and spallation of oxide layers [39]. TiO_2 and Ti_2O_3 oxide scale forms rapidly and can protect the substrate effectively in the lower temperature range, but reportedly is not stable and protective at very higher temperature. Secondly, void formation in Ti based coatings is quiet higher than alumina based coatings, which virtually leads to weak, porous and fragile oxide scales [37]. Chim et al. have also reported better tribological properties as well as higher corrosion resistance and better cutting performance of CrAlN than TiAlN coatings [43]. Hence by virtue of these facts, AlCrN coating has been proved to be a better option to protect the T91 boiler steel in the simulated boiler environment.

5. ACKNOWLEDGEMENT

The corresponding author would like to acknowledge I.K.Gujral Punjab Technical University, Jalandhar for providing the requisite platform for conducting the research work.

6. CONCLUSIONS

1. PAPVD coating process has been successfully applied to deposit AlCrN and TiAlN coatings on T91 boiler steel having dense, firm and uniform presence.
2. The T91 bare boiler steel has high spalling, sputtering and exfoliation of the scale from the substrate during cyclic hot corrosion studies.
3. The AlCrN coating has proved to provide better corrosion resistance than TiAlN coating against the oxidizing environment for 50 cycles by virtue of comparatively higher availability of protective Cr_2O_3 and Al_2O_3 phases along with firm and adhered availability of coating even after complete cyclic study.

4. Comparatively, lower corrosion resistance of TiAlN coating can be quoted due to the formation of porous, non-protective Ti_2O_3 oxide layer during initial cycles of the study.

7. REFERENCES

[1] Chatha, S. S., Singh, H. and Sidhu, B. S., High temperature hot corrosion behavior of NiCr and Cr_3C_2-NiCr coatings on T91 boiler steel in an aggressive environment at 750^0C, Surface & Coatings Technology, 2012, 206: p. 3839-3850.

[2] Kumar, M., Singh, H. and Singh, N., Production of nanocrystalline Ni-20Cr coatings for high-temperature applications, Journal of Thermal Spray Technology, 2014. 23(4): p. 692-707.

[3] Sidhu, T. S., Prakash, S. and Agrawal, R.D., Hot corrosion performance of a NiCr coated Ni-based alloy, Scripta Materilia, 2006. 55: p. 179-182.

[4] Kaur, M., Singh, H. and Prakash, S., High-temperature behavior of a high-velocity oxy-fuel sprayed Cr_3C_2 -NiCr coating, Metallurgical & Materials Transactions A, 2012. 43(8): p. 2979-2993.

[5] Rana, N., Jayaganthan, R. and Prakash, S., Stepwise depletion of coating elements as a result of hot corrosion of NiCrAlY coatings, Journal of Materials Engineering and Performance, 2014. 23(2): p. 1-15.

[6] Kaushal,G., Singh, H., and Prakash, S., Comparative high temperature analysis of HVOF-sprayed and detonation gun sprayed Ni-20Cr coating in laboratory and actual boiler environment, Oxidation of Metals, 2011. 76: p. 169-191.

[7] Chawla, V., Microstructural characteristics and mechanical properties of nanostructured and conventional TiAlN and AlCrN coatings on ASTM-SA210 Grade A-1 boiler steel, Corrosion, 2013. P. 1-14.

[8] Chawla, V., Chawla, A., Sidhu, B. S., Prakash, S. and Puri, D., Oxidation behavior of nanostructured TiAlN and AlCrN thin coatings on ASTM-SA213-T-22 boiler steel, Journal of Minerals and Materials Characterization Engineering, 2010. 9(11): p. 1037-1057.

[9] Luo, H., Goberman, D., Shaw, L. and Gell, M., Indentation fracture behavior of plasma-sprayed nanostructured Al_2O_3–13wt. %TiO_2 coatings, Materials Science & Engineering A, 2003. 386: p. 237-245.

[10] Grewal, J. S., Sidhu, B. S. and Prakash, S., High temperature erosion performance of nanostructured and conventional TiAlN coatings on AISI-304 boiler steel substrate, Transactions of Indian Institute of Metals, 2014. 67(6): p. 889-902.

[11] He, J. and Schoenung, J. M., Nanostructured coatings, Materials Science & Engineering A, 2002. 336: p. 274-319.

[12] Grosdidier, T., Tidu, A. and Liao, H. L., Nanocrystalline Fe-40Al coating processed by thermal spraying of milled powder, Scripta Materilia, 2001. 44: p. 387-393.

[13] Lin, J., Mishra, B., Moore, J. J. and Sproul, W. D., A study of the oxidation behavior of CrN and CrAlN thin films in air using DSC and TGA analyses, Surface & Coatings Technology, 2008. 202: p. 3272-3283.

[14] Marple, B. R., Voyer, J., Bisson, J. F. and Moreau, C., Thermal spraying of nanostructured cermet coatings, Journal of Materials Processing Technology, 2001. 117: p. 418-423.

[15] Shukla, V. N., Jayaganthan, R. and Tewari, V. K., Degradation behavior of nanostructured coatings deposited by high-velocity arc spraying process in an actual environment of a coal-fired boiler, JOM, 2013. 65(6): p. 784-791.

[16] Mittal, R. and Sidhu, B. S. Microstructural and mechanical properties of dissimilar weldment of ferritic and austenitic steels, in 3rd International and 21st technical sessions on welding and joining technologies, Interjoin-2016, Spain, 17-19 May 2016.

[17] Bala, N., Singh, H. and Prakash, S. High temperature oxidation studies of cold-sprayed Ni–20Cr and Ni–50Cr coatings on SAE 213-T22 boiler steel, Applied Surface Science, 2009. 255(15): p. 6862-6869.

[18] Rana, N., Mahapatra, M. M., Jayaganthan, R. and Prakash, S., High-temperature oxidation and hot corrosion studies on NiCrAlY coatings deposited by flame-spray technique, Journal of Thermal Spray Technology, 2015. 24(5): p. 769-777.

[19] Bourhis, Y. and John, C. S., Na_2SO_4 and NaCl induced hot corrosion of six nickel-base superalloys, Oxidation of Metals, 1975. 9(6): p. 506–528.

[20] Sidhu, B. S. and Prakash, S., Studies on the behaviour of stellite-6 as plasma sprayed and laser remelted coatings in molten salt environment at 900^0C under cyclic conditions, Journal of Materials Processing Technology, 2006. 172: p. 52-63.

[21] Mittal, R. and Sidhu, B. S., Microstructures and mechanical properties of dissimilar T91/347H steel weldments, Journal of Materials Processing Technology, 2015. 220: p. 76-86.

[22] Sidhu, B. S. and Prakash, S., Evaluation of the corrosion behaviour of plasma-sprayed Ni_3Al coatings on steel in oxidation and molten salt environment at 900^0C, Surface & Coating Technology, 2003. 166(1): p. 89-100.

[23] Bala, N., Singh, H., Karthikeyan, J., and Prakash, S., Performance of cold sprayed Ni-20Cr and Ni-50Cr coatings on SA516 steel in actual industrial environment of a coal fired boiler, Material Corrosion, 2013. 46(9): p. 783-793.

[24] Chatha, S. S., Singh, H. and Sidhu, B. S., The effects of post-treatment on the hot corrosion behavior of the HVOF-sprayed Cr_3C_2–NiCr coating, Surface & Coatings Technology, 2012. 206: p. 4212-4224.

[25] Chawla, V., Puri, D., Prakash, S. and Sidhu, B. S., Corrosion Behavior of Nanostructured TiAlN and AlCrN Hard Coatings on Superfer 800H Superalloy in Simulated Marine Environment, Journal of Minerals and Materials Characterization and Engineering, 2009. 8(9): p. 693-700.

[26] Mittal, R. and Sidhu, B. S., Oil-ash corrosion resistance of dissimilar T22/T91 welded Joint of super heater, Journal of Materials Engineering and Performance, 2015. 24(2): p. 670-682.

[27] Al-Hamid, Diverse scaling behavior of the Ni-20Cr alloy, Materials Chemistry & Physics, 2003. 80: p. 135-142.

[28] Mudgal, D., Kumar, S., Singh, S. and Prakash, S., Corrosion behavior of bare, Cr_3C_2-25%(NiCr), and Cr_3C_2-25%(NiCr)+0.4%CeO_2-coated superni 600 under molten salt at 900^0C, Journal of Materials Engineering and Performance, 2014. 23(11): p. 3805-3818.

[29] Ding, Y., Effects of elevated temperature exposure on the microstructural evolution of Ni(Cr)-Cr_3C_2 coated 304 stainless Steel,'' Ph.D. Thesis, University of Nottingham, 2009: p. 191.

[30] Mahesh, R. A., Jayagnthan, R. and Prakash, S., A study on the oxidation behaviour of HVOF sprayed NiCrAlY-0.4%CeO_2 coatings on super alloys at elevated temperature, Materials Chemistry & Physics, 2010. 119: p. 449–457.

[31] B. S. Sidhu, Studies on the role of coatings in improving resistance to hot corrosion and degradation, Ph. D. Thesis, Metallurgy & Materials Engineering. Department, IIT, Roorkee, India, 2003. p. 1-342.

[32] Das, D., Balasubramanium, R. and Mungole, M. N., Hot corrosion of Fe_3Al, Journal of Materials Science, 2012. 37: p. 1135-1142.

[33] Mittal, R. and Sidhu, B. S., Microstructural and mechanical characterization of different zones of T91/T22 weldment, International Journal of Surface Engineering and Materials Technology, 2014. 4(2): p. 45-49.
[34] Seiersten, M., and Kofstad, P., The effect of SO_3 on vanadate-induced hot corrosion, High Temperature Technology, 1987. 5(3): p. 115-122.
[35] Mittal, R. and Sidhu, B. S., Studies on microstructural properties of GTAW weldment of ferritic steels, Materials Forum, 2014, 38: p. 158-166.
[36] Kamal, S., Jayaganthan, R. and Prakash, S., Evaluation of cyclic hot corrosion behaviour of detonation gun sprayed Cr_3C_2–25%NiCr coatings on nickel and iron-based super alloys, Surface & Coatings Technology, 2009. 203: p. 1004–1013.
[37] Zandrahimi, M., Vatandoost, J. and Ebrahimifar, H., Pack cementation coatings for high-temperature oxidation resistance of AISI 304 stainless steel, Journal of Materials Engineering and Performance, 2012. 21(10): p. 2074-2079.
[38] Mishin, Y., and Herzig, C., Diffusion in the Al-Ti system, Acta Materialia, 2000. 48(3): p. 589–623.
[39] Sidhu, B. S., Puri, D. B. and Prakash, S., Characterization of plasma sprayed and laser remelted NiCrAlY bond coats and Ni_3Al coating on boiler tube steels, Materials Science & Engineering A, 2004. 368: p. 149-158.
[40] Kamal, S., Jayaganthan, R. and Prakash, S., Hot corrosion studies of detonation-gun-sprayed NiCrAlY+0.4%CeO_2 coated superalloys in molten salt environment, Journal of Materials Engineering and Performance, 2011. 20: p. 1068–1077.
[41] Willmann, H. Mayrhofer, P. H., Persson, P. O. A., Reiter, A. E.,Hultman, L. and Mitterer, C., Thermal stability of Al–Cr–N hard coatings, Scripta Materilia, 2006. 54(11): p. 1847–1851.
[42] Mittal, R., Goyal, L. and Sidhu, B. S., Study of corrosion behavior of SA213T91 boiler steel in the environment of air and molten salt of Na_2SO_4-60%V_2O_5 at 900^0C, International Journal of research in mechanical engineering & technology, 2013. 3(2): p. 58-63.
[43] Chim, Y. C., Ding, X. Z., Zeng, X. T. and Zang, S. Oxidation resistance of TiN, CrN, TiAlN and CrAlN coatings deposited by lateral rotating cathode arc, Thin Solid Films, 2009, 517: p. 4845-4849.
[44] Ding, X. Z., Tan, A. L. K., Zeng, X. T., Wang, C., Yue, T. and Sun, C. Q., Corrosion resistance of CrAlN and TiAlN coatings deposited by lateral rotating cathode arc, Thin Solid Films, 2008. 516: p. 5716-5720.
[45] Fujita, K., Research and development of oxidation, wear and corrosion resistant materials at high temperature by surface modification using ion processing, Surface & Coatings Technology, 2005. 196: p. 139– 144.